The 8th International Supercritical $CO_2$ Power Cycles Symposium
February 27 – 29, 2024, San Antonio, Texas
Paper 45

# Bearingless Motor/Generator Opportunities in $sCO_2$ Power Cycles

Takahiro Noguchi[a], WaiYan Chan[b], Nathan Petersen[b], Logan Rapp[c], Eric Severson[a]

[a] *University of Minnesota.* [b] *University of Wisconsin–Madison.* [c] *Sandia National Laboratories.*

## Abstract

Thermal power cycles using $sCO_2$ as a working fluid place extreme demands on their turbomachinery components and their electric motors/generators. In this paper, new system topologies for $sCO_2$ turbomachinery are proposed which take advantage of "bearingless" electric machine technology to improve performance. Bearingless motors/generators are a new type of electric machine which integrate the functionality of active magnetic bearings into the existing hardware of an electric motor/generator. The existing electromagnetic surfaces and materials are reused to enable controllable production of radial forces on the machine shaft. This is envisioned to improve hermetic direct-drive turbomachinery systems by either augmenting existing bearings (i.e., bearing assist) or replacing existing bearings (i.e., bearing removal). The state-of-the-art technologies for several bearing types (gas foil bearings, externally pressurized porous (EPP) gas bearings, and active magnetic bearings) and electric machines are reviewed to motivate the introduction of bearingless technology. Two system designs using bearingless machines are proposed and compared against existing commercial solutions in terms of maximum shaft weight, number of passthroughs into the hermetic environment, cost, and complexity. The proposed bearingless solutions have potential to enable a new generation of $sCO_2$ turbomachinery with improved reliability, reduced complexity, and lower cost. This paper shows that by transforming the motor/generator already present in turbomachinery into a bearingless motor/generator, the technical challenges involved with $sCO_2$ can be overcome without adding significant cost.

**Keywords:** Bearingless motor, $sCO_2$ power cycle, gas foil bearing, EPP gas bearing, magnetic bearing

## 1 Introduction

Thermal power cycles operating with supercritical carbon dioxide ($sCO_2$) as a working fluid were initially proposed as early as the 1960s. In recent years, with the advancements in heat exchanger development and an emphasis on achieving high thermal efficiency, the $sCO_2$ Brayton cycle has garnered significant attention from both researchers and commercial power cycle developers. This cycle offers several advantages, such as the ability to achieve high thermal-to-electrical efficiency from various heat sources (such as waste heat, nuclear, and concentrated solar), a small physical footprint, and requires no water to operate. These features collectively allows the $sCO_2$ Brayton cycle to become a compelling candidate in replacing the traditional steam Rankine cycle in thermodynamic power cycles [1].

In thermal power cycles, turbomachinery is used to convert energy from continually flowing fluid into mechanical/electrical energy via the dynamic action of turbines. Figure 1 shows a conventional turbomachinery system topology where the power grid, motor with a lubricated pump system, gearbox, and turbine/compressor are cascade-connected [2]. This enables connecting low-speed (e.g. 1800 RPM) motors/generators to high-speed compressors/turbines. All the components can be assembled separately and can come from separate vendors, making system design and maintenance easier. However, this configuration has many components which causes complexity and makes the physical footprint of the entire system large. The efficiency of this approach is limited due to the low-speed induction motor energy losses, gearbox

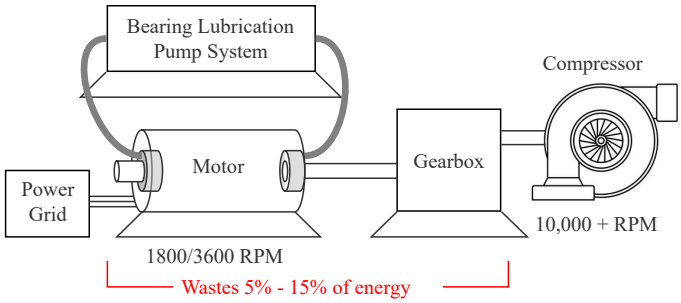


Fig. 1: Conventional turbomachinery system showing auxiliary bearing lubrication system and gearbox.

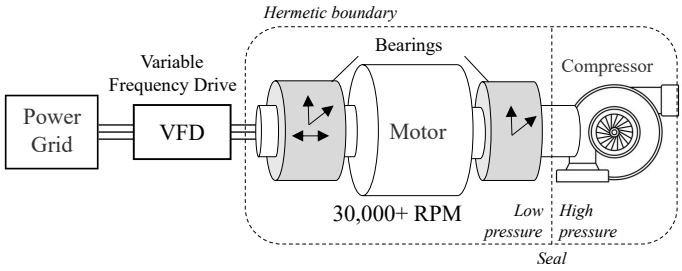


Fig. 2: Improved direct-drive hermetic turbomachinery system.

losses, and oil lubrication system energy losses (e.g., additional pumps). The motor and gearbox waste between 5% to 15% of energy. Conventional turbomachinery designs, like Fig. 1, are popular and are the mostly broadly used today. However, they have challenges of complexity, larger size, more components, and lower efficiency.

Recent technology advancements have made it possible to simplify the classical turbomachinery system design by reducing component count while simultaneously increasing system power conversion efficiency. High-speed motors coupled with variable frequency drives (VFDs) enable the motor and compressor to share the same shaft, removing the need for a gearbox. Figure 2 shows the improved system topology. By eliminating the gearbox, this direct-drive approach improves system lifetime and reliability [3]. Furthermore, VFDs enable high-speed motor operation above what is possible with line-driven motors. Turbomachinery systems have realized direct-drive operation by overcoming several challenges in high-speed machines, such as improvements of loss per volume, bearing stiffness and lifetime, rotor dynamics and vibration, cooling, high switching stress for power electronics [4]. For example, it is well established that the switching frequency of the VFD must be higher (>10x) than the fundamental frequency of electric motors. Historically, this set a limit on the maximum motor operating speed. However, recently, wide bandgap (WBG) semiconductors have been developed which are capable of switching much faster than standard insulated-gate bipolar transistors (IGBTs) [5]. This unlocks new possibilities for electric machine operating speeds.

Ongoing hardware development for $sCO_2$ systems have placed emphasis on machines with sub-1 $MW_e$ capacity. At this power level, radial turbines and compressors, along with permanent magnet alternators, can be effectively utilized. This configuration enables the adoption of a turbine-alternator-compressor (TAC) architecture, where the turbine, alternator, and compressor are integrated on a single shaft [6]. An example TAC design is shown in Fig. 3. By utilizing the TAC configuration, the shaft seal between the turbine and the generator can be eliminated. When combined with a scavenger pump, this configuration enables the recovery of any leakage beyond the labyrinth seals in the motor cavity. As a result, this arrangement facilitates the recovery of leakage and reducing the pressure in the motor cavity, leading to minimal loss of working fluid to the atmosphere and excessive windage losses in the rotor. From a system level, the most compact topology

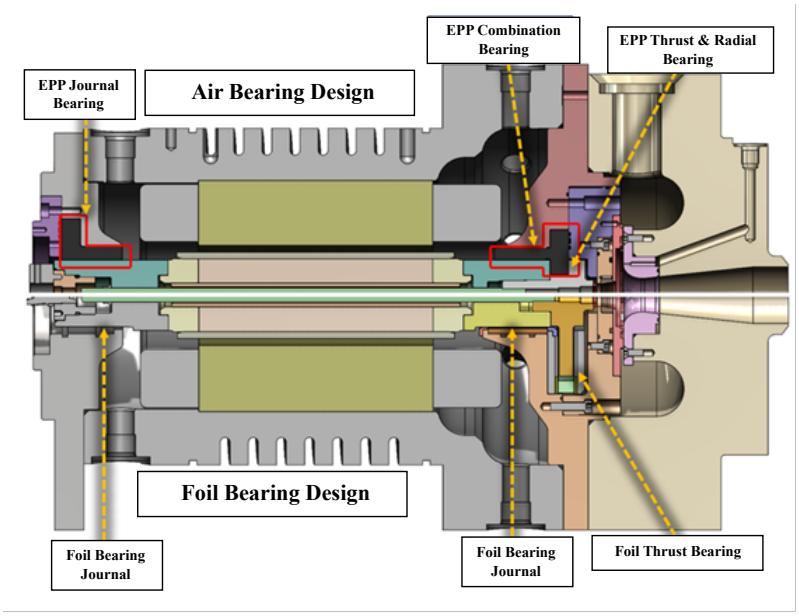


Fig. 3: Sandia National Laboratory $sCO_2$ turbogenerator prototype. Bottom half of the figure shows the current design with gas foil bearings, labyrinth seals and a permanent magnet rotor for the TAC design. In contrast, the top half shows a revised design with EPP bearings.

uses a hermetic design where the electric generator is exposed to the working fluid. In the hermetic cavity, both the high-speed direct drive with a turbine and the compressor wheels are in the sealed environment. A high-pressure environment in the compressor wheel side poses challenges of windage loss, even within the lower pressure cavity. This concept eliminates the need for lubricants, but at the same time, the motor must be driven in an oil-free environment.

## 2 Bearing and Electric Machine Challenges in sCO2

The inherent high pressure and temperature of $sCO_2$ working fluid leads to challenges for the electric generator integration. This section presents two challenges in hermetic design: 1) high pressure leading to viscous windage losses and bearing failure; 2) high temperature leading to thermal management challenges in electric machines.

As described in Section 1, the high operating pressure that comes with the $sCO_2$ environment creates notable challenges for turbomachinery. High pressure leads to viscous windage losses on the surfaces of the rotating machinery. While designers minimize this by placing the bearings and motors inside a lower pressure cavity, viscous losses remain a significant factor in the design [7]. Furthermore, the high pressure environment leads to extreme dynamic bearing loads. Both of these aspects are further complicated by the hermetic environment requiring the use of oil-free bearing types (gas or magnetic bearings) which have lower specific load capacities are require larger diameters than contact bearings. This leads to challenges for designers trying to minimize the bearing surface area and diameter (for viscous losses) while also ensuring sufficient force capacity (to prevent bearing crashes and eventual failure from load transients). Detailed oil-free bearing technology considerations will be discussed later, in Section 3.

The other primary challenge is high operating temperature. In order to achieve high thermal-to-electrical power conversion efficiencies, there is a need to operate with a high turbine inlet temperature. For a $sCO_2$ system, the compression work can be reduced by taking the turbine temperature near 700°C, which results

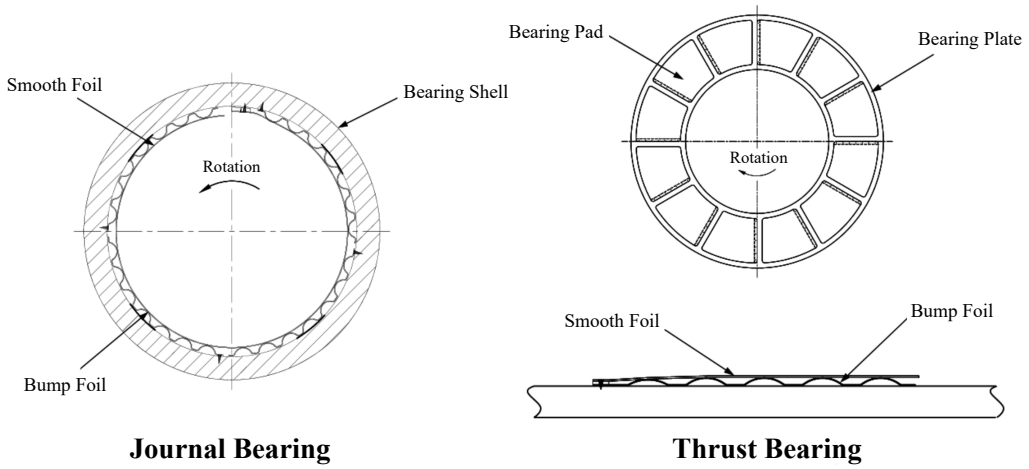


Fig. 4: Typical construction for gas foil journal and thrust bearings, adopted from [10].

in a significant higher efficiency of approximately 50% [8]. However, under high temperature environments, permanent magnets run the risk of demagnetization and can permanently alter the electric machine's performance. This makes thermal management near the shaft seals and bearings a critical challenge, especially for temperature sensitive components such as magnetic bearings and the permanent magnets located on the rotor.

## 3 Commercial Bearing Solutions

Three distinct variations of bearing systems used in combination with conventional electric machines are examined in this section. Focus is specifically placed on oil-free bearing technologies suitable for operating under $sCO_2$ hermetic environments. These include: 1) passive gas foil bearings, 2) EPP gas bearings, and 3) magnetic bearings.

### 3.1 Gas Foil Bearings

Gas foil bearings are a type of hydrodynamic bearing that leverage the gas pressure generated from compliant, spring-loaded foils to provide contact-free support under high-speed shaft rotation [9]. Functioning solely through mechanical means, these bearings operate passively without the need for active feedback control. In addition, due to their hydrodynamic nature, gas foil bearings do not require any cable or hose passthroughs into the motor and bearing cavity. This feature, coupled with their operational simplicity, contributes to reduced system complexity and a cost-effective solution in comparison to EPP and active magnetic bearings. Typical construction for gas foil type radial and thrust bearings is shown in Fig. 4.

Over the past two decades, researchers have constructed numerous $sCO_2$ turbomachinery prototypes using gas foil bearings. A prominent example is the 125 $kW_e$ scale demonstration systems installed in the $sCO_2$ Brayton loop at the Sandia National Laboratories (SNL) [6]. The cross-sectional view of the SNL TAC unit is shown in Fig. 3. The prototype integrates a TAC design with radial gas foil bearing on each end of the rotor shaft, with an additional thrust foil disk bearing on one end to provide axial support.

While the gas foil bearing technology poses as a promising option for $sCO_2$ turbomachinery applications, it comes with its drawbacks. One major drawback is its inability to generate adequate support during startup and shutdown events. Due to the operating principles of gas foil bearings, the rotor shaft must reach a certain threshold speed for the rotor to achieve "lift-off." During the start-up or shutdown process, friction is gener-

ated when the rotor slides on the bearing foil, leading to wear and degradation of the foil. Over time, after numerous cycles, the bearings eventually wear out and require maintenance. This is especially concerning for thrust-type foil bearings with a low thrust capacity, and failures have been recorded in the SNL sCO2 prototype. Apart from wear, heat generation of this type of bearing is also a concern. An $sCO_2$ turbogenerator prototype that has a design architecture similar to SNL's prototype at the Naval Nuclear Laboratory has found the rotational speed of the TAC unit needs to be limited at 60 kRPM to prevent excessive heat generation due to the bearings' exposure to the $sCO_2$ pressure boundary [11]. In addition, due to its passive nature, this type of bearing lacks ability to control its properties dynamically, which is important in improving rotordynamics [12]. Furthermore, the fabrication of the compliant foil structure for this type of bearing also brings additional challenges to its larger scale implementation [13]. While gas foil bearings offer promise for $sCO_2$ turbomachinery applications, their limitations in generating adequate support at startup/shutdown and their passive nature, along with concerns about wear and heat generation, call for careful consideration in their use.

### 3.2 EPP Bearings

The externally pressurized porous (EPP) bearing is a type of aerostatic bearing that relies on pressurized gas to provide non-contacting support [14]. The externally pressurized gas is channeled through a porous material (typically carbon graphite) and subsequently introduced into the gap between the porous and supporting surfaces. This process results in a thin micron-scale gas film that effectively acts as a lubricant within the clearance between the surfaces, allowing the bearing to operate in an ultra-low friction manner. Research literature finds that the friction factor of this type of bearing can achieve as low as 0.019, resulting in nearly friction-free operation [15].

Various existing EPP bearing products, such as the concave and convex porous carbon radial bearing pads shown in Fig. 5a [16], can be assembled together to form a full radial bearing to provide radial support for rotary machinery, as shown in Fig. 5b. Additionally, various manufacturers have also designed EPP thrust bearings, which in combination could provide five degrees of freedom support.

An important advantage EPP bearing has over the gas foil bearing is its aerostatic nature, meaning it has ability to suspend the rotor shaft just by using externally pressurized gas. Such advantage eliminates the reliance on rotor rotation to generate suspension support, resulting in minimal frictional force generated during startup/shutdown events. The constant pressurization also provide additional benefit in acting as a shaft seal to prevent the backflow of fluids during operation; crucial for hermetic $sCO_2$ system. Despite the benefits, in order to operating this type of bearing, additional infrastructure such as pressurized gas pump and passthroughs are required. To mitigate such issue, one solution is to utilize the high pressure $sCO_2$ fluid as the lubricating fluid for the EPP bearing. This solution is proposed in the new design iteration of the SNL $sCO_2$ turbogenerator prototype shown in the top half of Fig. 3. This method of using the $sCO_2$ fluid to support the EPP bearing comes at the expense of a slight decrease of thermal efficiency, and a pressurized pump is still required for system startup.

Despite the advantages, EPP bearings have the reputation of limited damping capacity. In recent research, an externally pressurized *compliant* gas bearing topology has been proposed and designed by GE Research and Oak Ridge National Lab [17]. The proposed design utilizes additive manufacturing to fabricate an externally pressurized gas bearing that is flexibly mounted with hermetic squeeze film dampers (HSFD). With this design, researchers aim to overcome the limitations of low load and damping capacity inherent in traditional gas bearing technology and demonstrate a notable increase in load-carrying capability for $sCO_2$ application [18]. Experimental work was performed on this new topology and thrust force measured was able to effectively scale proportionally with supplied pressure [19]. Test rig for the prototype is currently underway and more testing will be performed on this topology.

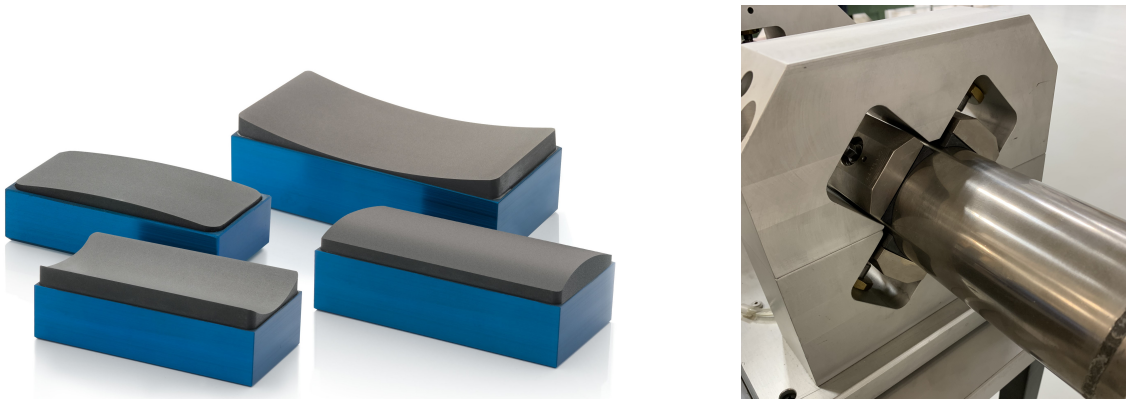

(a) (b)

Fig. 5: EPP bearing products: (a) EPP carbon pads with various concave and convex geometries for inner/outer bore support, adopted from [16]. (b) EPP radial bearing comprised of four porous carbon pads.

Despite its success in various applications today, the EPP bearing technology has yet to penetrate the turbomachinery industry, and further research and development is required to mature the technology for high-power turbomachinery applications.

### 3.3 Active Magnetic Bearings

Active magnetic bearing (AMB) technology is a type of bearing that relies on real-time controlled electromagnetic forces to generate shaft support without any physical contact [20]. AMBs employ electromagnets and active controllers to constantly adjust and maintain the position of the rotor. The rotor displacements are measured by position sensors that feed into programmable controllers, allowing real-time adjustments to the magnetic forces. This process ensures precise control over the rotor's position.

An example where AMBs have found success in $sCO_2$ application is the Supercritical $CO_2$ Brayton Cycle Integral Experiment Loop (SCIEL) at the Korea Atomic Energy Research Institute (KAERI). The research team at KAERI was able to achieve stable operation of maximum 40 kRPM for the $sCO_2$ compressor under supercritical environment with two radial and one axial AMBs [21]. Additionally, MAN Energy Solutions Schweiz in Switzerland implemented a hermetically sealed $sCO_2$ motor/compressor using AMBs for an industrial heat pump with targeted temperature of 200°C [22].

Unlike passive bearings, AMBs offer advantages such as consistent levitation stiffness and damping under wide range of speed using active controllers. The active nature of AMBs provides further ability in mitigating rotor imbalance due to thermal gradient, which is achieved by allowing rotor rotation around its inertial axis using synchronous control. Such control is critical for reducing vibration forces on the housings and ensuring system stability [23]. In addition, the ability to measure both steady-state and dynamic forces exerted by the bearings further enhances the benefits for system health monitoring. To implement systems with AMBs, position sensors and real-time controllers are required. As a result, the number of passthroughs and cost required is higher in comparison to the passive bearings. AMBs also require more shaft length for the rotor, which can negatively impact rotordynamic performance. A research group at the Korea Advanced Institute of Science and Technology (KAIST) has also found that the property change of $sCO_2$ near its critical point can affect the performance of AMB by causing disturbance to the $sCO_2$ lubrication force on the rotor shaft [24]. The control complexity, combined with the cost and shaft length limitation, increases the difficulty of integrating AMBs into $sCO_2$ turbomachinery applications

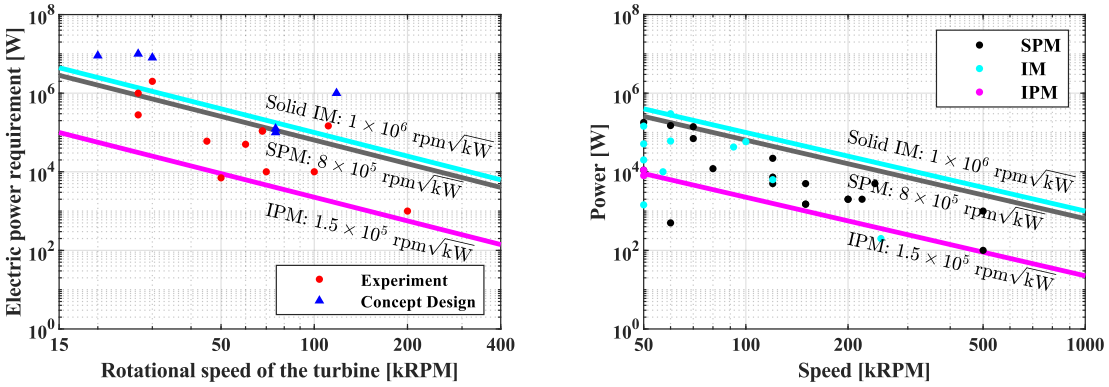


Fig. 6: Published speed-power: (a) $sCO_2$ turbomachinery designs, data from [25–29]; (b) high speed induction motors (IM) and permanent magnet motors (surface (SPM) and internal (IPM)), data from [30].

## 4 Existing High Speed Motor Solutions

As shown in Section 1, $sCO_2$ TACs require a high-speed direct drive motor/generator. This section reviews high speed motor system technology (electric machines and drives) for use with $sCO_2$ turbomachinery. To quantify the speed and power range required of the electric motor system, a summary of the speed and power ratings for $sCO_2$ turbomachines published in literature is shown in Fig. 6a. While these designs represent a variety of architectures, the data gives a representation of what would be required of the electric motor/generator if the system were to be realized in the direct-drive configuration of Fig. 2: maximum rotational speeds in the range of 27 - 100 kRPM and power rating in the range of 10 kW - 8 MW, with most designs requiring 50 - 300 kW.

While high speed electric motor technology is commercially available within this range, it is largely developed on a custom basis, unlike the “catalog” motors that can be found at speeds of 3600 RPM and lower. The high speed motor technology is typically based around induction motors (IM) and permanent magnet (PM) motors, operated with variable speed motor drives, all of which are now reviewed in this section.

### 4.1 High Speed Motors

IMs are the most prevalent type of electric motor, frequently referred to as “the workhorse of industry” because they are low cost and simple to use. The rotor of these machines is implemented as a conducting structure—typically either an aluminum or copper squirrel cage or a random wound rotor winding inserted into steel laminations. IMs developed for high speeds typically use what is referred to as a “solid rotor,” where the rotor is a single piece of magnetic steel [30,31]. While this can degrade the machine’s efficiency, it enhances the rotor strength, resulting in higher achievable tip speeds and power density. For further information on high speed IMs, the reader is referred to [32].

In contrast, PM motors are used in industry for premium efficiency and higher power density, but come at a significantly higher price point. The PM rotors used for high speeds nearly always use rare-earth permanent magnets, which can pose supply chain challenges. Rare-earth magnets are composed of either NdFeB or SmCo. Of these, NdFeB magnets are widely used in high speed motor designs, but are prone to irreversible demagnetization at high operating temperatures and therefore necessitate advanced cooling to function reliably at the high operating temperatures of $sCO_2$ turbomachinery. Alternately, SmCo magnets have better

temperature stability and may prove to be a more cost-effective option. A detailed overview of high speed PM designs can be found in [30].

The speed-power capability of electric motors is of particular relevance to the development of direct drive $sCO_2$ turbomachinery. It is often assumed that for any given desired rotational speed, an electric motor can be designed for any arbitrary power rating. However, this is not true. Each motor technology has limitations on the maximum power than can be achieved as a function of speed based on the structural integrity of the rotor, dynamics (critical speeds), and cooling requirements. This concept is developed and explored in [30, 33] for different motor types. Figure 6 shows the empirical speed-power capability limits of IM and PM motors (solid lines) alongside published speed-power data of actual designs (data markers). The solid rotor (IM) has the highest capability ($1 \times 10^6$ rpm$\sqrt{\text{kW}}$) while the surface PM (SPM) motor is lower ($8 \times 10^5$ rpm$\sqrt{\text{kW}}$) and the internal PM (IPM) motor is lowest ($1.5 \times 10^5$ rpm$\sqrt{\text{kW}}$).

In Fig. 6a, the motor speed-power limit lines are overlaid on the speed-power ratings of existing $sCO_2$ turbomachines. From this plot, it is evident that the most demanding $sCO_2$ turbomachines exceed the capabilities of today's high speed motors. The markers in Fig. 6a that are above the "Solid IM" line correspond to turbomachinery architectures that use a gearbox to step the shaft speed down to allow the use of a lower speed motor/generator. This plot provides evidence of the challenges of integrating electric motors into $sCO_2$ direct drive turbomachinery, and motivates the need for innovative motor solutions.

### 4.2 High Frequency Motor Drives

The operation of electric motors/generators beyond grid-tied frequencies (i.e., 50/60 Hz) generally requires motor drives. Variable frequency drives (VFDs) are electronic devices which convert fixed-frequency AC grid power into variable-frequency AC power to drive AC motors—the speed of the motor is tied to the power frequency. VFDs are built using power electronic switching devices, e.g., Si MOSFETs or IGBTs. While "small" VFDs are commercially mass produced and have seen significant market penetration, there is a lack of availability for VFDs rated at significant power levels combined with high fundamental power frequencies (e.g., 600+ Hz). New wide bandgap (WBG) semiconductor devices (e.g., SiC MOSFETs) are necessary for VFDs in turbomachinery applications due to high switching frequencies and increased operating temperatures. Unfortunately, WBG devices are more expensive and prone to electromagnetic interference (EMI) problems [34] which make adopting them challenging. In addition to the power electronic issues, the control algorithms for high speed motors are also challenging. During high-speed operation, the typical modeling assumptions for standard VFD software no longer hold true due to nuances in how the digital processor interacts with the rotating machinery. The default drive software of common VFDs is usually not capable of driving ultra-high-speed loads. Careful design, calibration, and tuning of the motor drive algorithms when paired with high-speed motors is crucial for stable operation.

To complicate matters, the USA and the EU restrict the export of VFDs with frequencies above 600 Hz (called "high-frequency" drives), which simultaneously restricts the use of high-speed motors. Due to the export control regulations, most manufacturers only sell drives that operate below 600 Hz. This directly limits motor operating speed, for example, a 2-pole motor operating at 600 Hz is only 36 kRPM. However, based on Fig. 6a, the current state-of-the-art $sCO_2$ turbomachinery requires operating speeds well in excess of 36 kRPM, e.g., 100+ kRPM. These factors contribute to the fact that high-speed motors and drives tend to be custom per each customer application and limit the ease of adoption for high-speed machinery.

## 5 Bearingless Motor Technology

Over the past four decades, several research institutions have developed an electric motor technology that is able to control radial electromagnetic forces on the rotor shaft. This technology is referred to as a

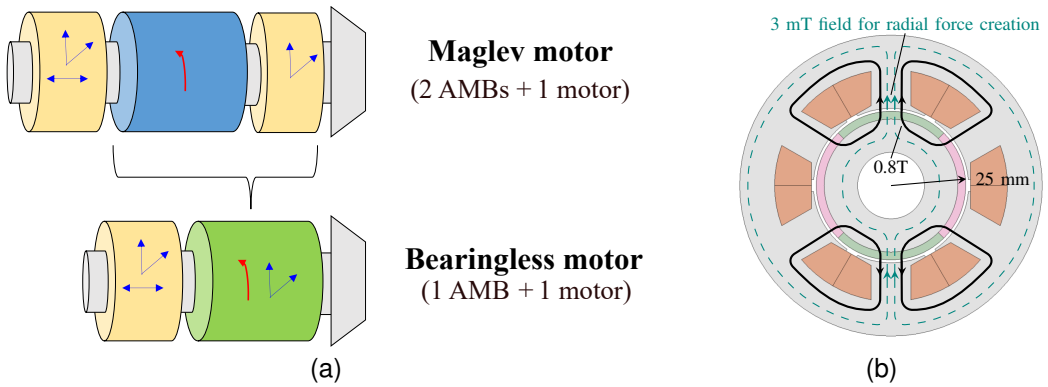


Fig. 7: Bearingless motor: (a) shown as a combination of traditional motor and a radial AMB; (b) fields used to create a force towards the top of page with a high speed 4-pole PM rotor.

"bearingless" motor because it can potentially eliminate bearings from a motor system. It can also be used in combination with the existing bearings in the system to enhance performance. For $sCO_2$ turbomachinery systems that already have motor/generator components, this technology offers a pathway to solve key bearing challenges without having to significantly modify the system hardware. This section will introduce bearingless motors and describe their potential impact for turbomachinery systems. An overview of the technology is presented, including a brief history, review of research literature, and discussion on the potential to reach the power and efficiency required by $sCO_2$ applications. The section presents evidence that bearingless technology has recently matured to a level that makes it a compelling solution for turbomachinery systems.

### 5.1 Overview

The fundamental feature of an electric motor that makes it "bearingless" is the capability to create and control radial forces on the shaft in addition to torque [35]. A bearingless motor provides the functionality of both a motor and a radial AMB actuator, but within a single machine, as depicted in Fig. 7a. This is accomplished by introducing a “suspension" magnetic field into the airgap of a standard electric motor. Figure 7b depicts this for an example PM rotor and illustrates that only a very small field (3 mT in this case) needs to be added to completely offset the rotor weight. This same principle can be extended to make any type of motor bearingless (i.e., IM, IPM, synchronous reluctance), though the nuances of doing this effectively are significant and have taken time to mature, as will be outlined in the following subsections.

The fact that only minute changes to the electric machine design are required to create significant shaft forces makes bearingless motors an intriguing technology for application spaces that require oil-free bearings, like $sCO_2$. Figure 7a provides an overview of plausible turbomachinery configurations using AMBs (top) and a bearingless motor (bottom). Here, the bearingless motor is able to replace one of the radial magnetic bearings and thereby simplify the system and reduce the required shaft length. System configurations for $sCO_2$ will be proposed in detail in Section 6.

### 5.2 History

This section briefly reviews the history of bearingless motors and key trends in the technology’s development. Concepts of creating both magnetic bearing forces and motor torque on a shaft can be traced back to the 1970s [36], with subsequent literature considering specialized cases of making shaft force and torque. In 1989, a general concept for the bearingless motor was proposed by Chiba, et al in [37], and further refined

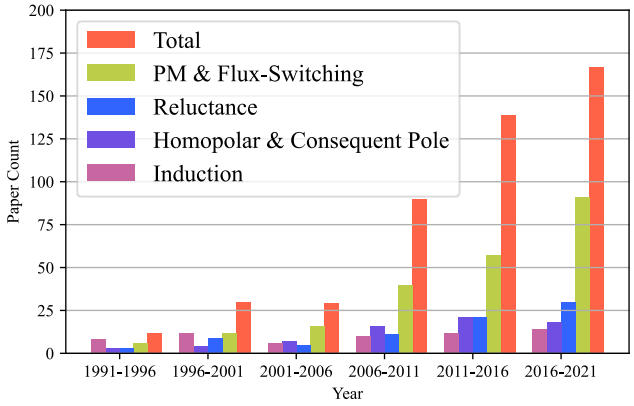


Fig. 8: Bearingless motor literature review from [46], number of papers with experimental results published.

in seminal paper [38], which show that any type of motor can be transformed into a bearingless motor. Since then, researchers have explored bearingless versions of several different types of motors. Examples include surface-mounted PM motors [39], IM [40, 41], synchronous reluctance motors (SynRM) [42], and switched reluctance (SwR) motors [43].

Figure 8 shows the number of papers published on bearingless motors with experimental results by year. The research field is clearly growing rapidly, indicating intense interest as the technology has matured and gained increasing capabilities. From this figure, it is evident that the most popular type of bearingless motor is the PM machine. Investigations into bearingless versions of IMs represent the lowest share of publications, despite this being the most common type of motor used in industrial applications. This is likely because the IM has proven to be the most difficult machine to make bearingless due to the suspension magnetic field interacting with the conductive rotor, resulting in degraded motor performance. However, recent research into a new IM rotor structure (“pole-specific" rotor) offers a potential solution [44, 45].

Research has also focused on different system topologies, as reviewed in [46, Section III-A]. The two most common configurations include the so-called “slice" motor and the shafted configuration depicted in the bottom of Fig. 7a. The slice motor configuration features a large diameter to axial length ratio so that the rotor’s axial and tilting movements are passively stabilized magnetically [47]. This configuration has led to notable commercial success through Levitronix GmbH as a compact pump for an artificial heart as well as for hygienic processes in the semiconductor, pharmaceutical, and chemical industries. However, the bearingless slice motor concept is only able to be developed for low power ratings and has limited performance [48], making it not suitable for industrial-scale turbomachinery. Shafted configurations of bearingless motors (Fig. 7a) have been successful at reaching more significant power levels. A publication from 2000 [41] details test results of a 30 kW bearingless induction motor and in 2011, 30 kW test results were presented for a bearingless surface PM machine [49]. The current record for high power test results was set by a 2020 publication [50] at 60 kW with a bearingless buried PM machine.

Reaching both high power and efficiency has remained a critical challenge for bearingless motor technology. Figure 9 shows the achievable performance published in literature through 2021 with an overlay of the IE4 efficiency curve. Most research prototypes have not met the IE4 efficiency standard, which is presumably a prerequisite for use in energy applications such as $sCO_2$ turbomachinery. Literature has largely attributed this low performance of bearingless motors to a lack of careful machine design optimization and the use of stator winding structures that limit achievable performance [46]. Recent research on this front has focused on developing stator windings where the same coils can be used for creating both motor torque and suspension forces [51, 52]. These “combined” windings allow the bearingless drive electronics to dynamically adjust how much of the machine’s capacity is allocated to creating torque or force at run time, in response to operating

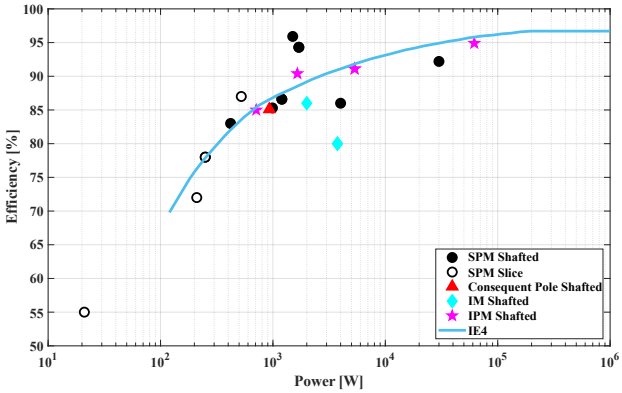


Fig. 9: Bearingless motor literature review from [46], efficiency of experimental prototype test results.

conditions such as surge or passing through a critical speed. It was shown in [53] that many standard motor windings can be transformed into bearingless combined windings by simply making additional winding end connections available to the drive electronics. This means that conventional motor manufacturing processes and supply chains can be used, and also makes it possible to easily convert conventional motor/generator designs into bearingless motors.

For more information on the basic operating principles, control strategy, and applications of bearingless motors, the reader is referred to [35].

### 5.3 Required Performance for Turbomachinery

Successfully introducing bearingless motors into turbomachinery applications, such as $sCO_2$ thermal power cycle systems, requires that bearingless machines reach power levels in excess of 100 kW (as reflected in Fig. 6a) with energy conversion efficiency that meets the IE4 efficiency standard. While there are not currently experimental demonstrations at this level in published literature, there are now numerous design studies that indicate feasibility. These case-studies leverage recent advancements in bearingless motor research outlined in Section 5.2, including combined windings, design optimization, and pole-specific rotors.

Examples of significant power, high efficiency bearingless motor studies include [54], which characterizes the design space of 50 kW bearingless PM generators at 25 and 100 kRPM that use combined windings through multi-objective optimization. The authors find designs capable of exceeding 97% efficiency at full load while using the bearingless motor's force capability to support the rotor weight. In [55], a detailed multi-physics design analysis is presented for a pair of 80 kW, 30 kRPM bearingless PM motors with combined windings used for a heat pump. The study finds an efficiency of 95.6% and that the bearingless configuration is able to reduce the shaft length as compared to a magnetic bearing configuration. In [45], a case study of a 100 kW, 30 kRPM bearingless IM with a pole-specific rotor and a combined winding is presented which achieves a modeled efficiency of 96.8%. Further scaling of bearingless motors up to 280 kW is considered in [56]. These investigations have all happened in university research laboratories, where high power experimental validation is inherently challenging to accomplish.

### 5.4 Required Electronics and Sensors

As explained in Section 5.2, transforming a motor/generator into a bearingless motor requires only small changes to the electric machine design. However, additional electronics and sensors are required to actuate the bearingless motor. In typical configurations, an additional three phase drive is required for creating

magnetic forces. This inverter is usually sized for a power rating that is 1-2 orders of magnitude smaller than the motor/generator drive electronics [35], making its additional cost minimal. If the bearingless motor is actively regulating the shaft's radial displacement, proximity probes (of the same type used for AMBs) are required for feedback control. Section 6 proposes a use-case for bearingless motors in turbomachinery where proximity probes are not required.

## 6 Proposed Solutions

This section proposes and explores system configurations that use a bearingless motor to improve the performance of $sCO_2$ turbomachinery. The proposed premise is to transform the motor/generator that is already present in the turbomachine into a bearingless motor and operate it in a manner that solves critical challenges with existing bearing solutions described in Section 3. Two fundamental approaches are considered—using the bearingless motor to 1) replace one of the radial bearings or 2) supplement or enhance the bearings.

In the approach of using a bearingless motor to supplement existing bearings, the bearingless motor effectively takes the role of unloading the bearings. This can be in the form of providing static forces or dynamic forces. In the case of static unloading forces, the bearingless motor can be thought of as a "weightless" motor, where it makes a constant magnitude and direction force to oppose gravity. In this manner, the bearingless motor is operated without need for any rotor displacement feedback (no proximity probes required). This makes static unloading a particularly easy and low-cost solution to implement. No additional passthroughs or sensors are needed within the motor cavity. The only change is to the stator winding of the machine and the drive electronics operating the machine.

When used for dynamic forces, the combined winding described in Section 5.2 is a particularly important feature, as it allows the machine's capacity to be dynamically adjusted between creating torque and force. In turbomachinery systems, the peak transient forces typically occur during surge events, where the electric motor is operating at a low power (torque) point, and therefore has excess capacity available that the combined winding can use for creating shaft forces. Conversely, during times when low dynamic loading is present, the combined winding can direct the full capacity of the machine to motor operation. Additionally, by actuating dynamic forces on a shaft that is already supported by bearings, the bearingless motor is able to disrupt flexible bending modes and allow the shaft to safely reach higher rotational speeds. Finally, when used with gas foil or EPP bearings, the bearingless motor can provide insights into the vibrations present on the shaft which can be used for diagnostic or health monitoring purposes.

From this discussion, it is evident that there are many plausible and advantageous architectures for integrating and using a bearingless motor in $sCO_2$ turbomachinery. This section will now propose and evaluate two distinct configurations that the authors believe to be promising.

### 6.1 Static Unloading of Gas Foil Bearings

The first proposed configuration is to use a bearingless motor to provide static unloading of gas foil bearings, as illustrated in Fig. 10a. Section 3.1 identified that one of the critical shortcomings of foil bearings is the wear that occurs on the bearing surfaces during start up leading to premature bearing failure and limiting the maximum shaft size (power rating) that the foil bearings can be used with. By operating the bearingless motor as a weightless motor, the foil bearing will experience significantly less wear, thereby extending its lifetime and allowing it to be used in higher power systems.

Of particular note here is the relative simplicity and low cost nature of this solution. The foil bearing system described in Section 3.1 requires no passthroughs into the motor/bearing cavity apart from the motor phases and no auxilliary hardware. These aspects are maintained when the bearingless motor is used to

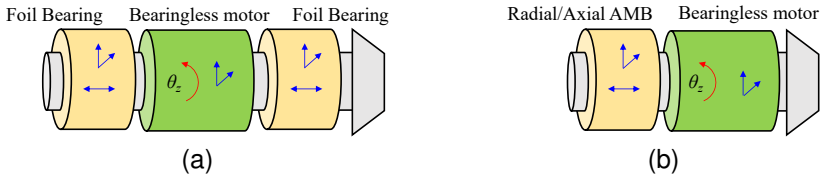


Fig. 10: Configurations of supplementing conventional bearing technology with bearingless machine: (a) bearingless motor + foil bearings; (b) bearingless motor + combined AMB.

provide static unloading. The only additional components required is a set of low power drive electronics, which can reside outside of the hermetic environment.

Section 3.1 also noted that limitations on thrust load capacity has been a challenge of foil bearings. Recently, bearingless motor researchers have begun exploring concepts to add either thrust load capacity or damping through control of field weakening current [57], reluctance forces [58], and a passive solution of incorporating an additional, short-circuited stator coil [59]. While these techniques are currently at early concept stages, if successful they could offer further advantages to this configuration, while not requiring additional passthroughs.

### 6.2 Replacement of Radial AMB

The second proposed configuration is to use a bearingless motor to replace a radial AMB in a completely magnetically levitated turbomachine, as shown in Fig. 10b. Section 3.3 identified that the critical challenges of AMBs for $sCO_2$ turbomachines include their high cost, high number of passthroughs, and the amount of shaft length that they require. By using the bearingless motor to eliminate the one radial bearing actuator (and it's corresponding cost, passthroughs, and shaft length), these challenges are at least partially mitigated.

The bearingless motor is able to provide identical force capabilities as the magnetic bearing it is replacing. This means that all of the inherent advantages of AMBs are preserved, most notably the ability to program a desired dynamic stiffness and damping. Further, by using a combined winding the bearingless motor will almost certainly have a higher peak force capacity as compared to the AMB it is replacing. This is because AMBs are typically sized for a peak force of 2.5 times their gravitational loading [20], whereas bearingless motors can produce upwards of 20 - 30 times their gravitational loading when the torque capacity is fully redirected to creating bearing forces [60].

### 6.3 Comparison of Commercial Bearings and Proposed Solutions

This section compares the relative performance of the bearing solutions summarized in Section 3 with the proposed bearingless motor solutions presented in Section 6.1 and 6.2. This comparison is presented in Table 1, where each row is a critical feature and each column is one of the potential bearing approaches. The three bearing solutions of Section 3 are the left-most columns, under the heading of "Conventional Motor", the solution of Section 6.1 is under the "Gas Foil" heading on the right side, within "Bearingless Motor," and the proposed solution of Section 6.2 is under the "Magnetic" heading on the far right. The critical features are largely self-explanatory, but note that "Active / Passive" refers to whether the shaft is supported via active feedback (i.e., AMBs) or passive (i.e. gas as a lubricant). All of the critical features within a bearing technology are given a rating relative to the other bearing technologies.

From this table, the gas foil bearing solution of Section 3.1 is evident as the simplest, least expensive, but lowest performance. In contrast, the AMB solution of Section 3.3 is the most complex, expensive, and highest

Table 1: Comparison table for existing commercial and proposed solutions.

| | **Conventional Motor** | | | **Bearingless Motor** | |
|---|---|---|---|---|---|
| | ***Gas Foil*** | ***EPP*** | ***Magnetic*** | ***Gas Foil*** | ***Magnetic*** |
| **Max. Shaft Weight** | Low | High | High | High | High |
| **# of Passthrough** | Low | Medium | High | Low | Medium |
| **Cost** | Low | Medium | High | Low | Medium |
| **Complexity** | Low | Low | High | Medium | High |
| **Active** / **Passive** | Passive | Passive | Active | Passive | Active |

performance. The proposed approaches of introducing a bearingless motor temper the shortcomings of each of these solutions, while maintaining their strengths. In particular, the solution of Section 6.1 offers notable gains (ability to support significantly higher shaft weight), while still maintaining a relatively simple system. The solution of Section 6.2 presents itself not as providing performance gains, but rather as reducing the number of passthroughs and cost. In summary, both of the proposed bearingless motor approaches have potential to result in a more functional, flexible, and easier to integrate motor / bearing solution for developing a direct drive $sCO_2$ turbomachine than a purely traditional approach to the bearings and motor.

## 7 Conclusion

The recent wave of interest from both research and commercial organizations in thermal power cycles using $sCO_2$ has highlighted the need for more capable electric machinery. Due to the combination of high rotating speeds and high power levels, today's electric motor and generator technology is not capable of handling the most demanding $sCO_2$ turbomachinery designs. State-of-the-art topologies such as the turbine-alternator-compressor require direct-drive hermetic electric machines with tightly integrated bearings capable of handling extreme dynamic loading. Existing commercial bearing and motor solutions struggle to meet the demands of oil free and high temperature operation while maintaining low cost. Bearingless motor technology may potentially be the key to enabling $sCO_2$-based hermetic turbomachinery due to its ability of adding versatility to existing electric machinery without using additional space. Two proposed solutions are presented: 1) static unloading of gas foil bearings, and 2) replacement of radial active magnetic bearings. Both solutions have the potential to improve the performance of their accompanying bearing technology to a level admissible for the hostile $sCO_2$ environment. For power generation using $sCO_2$-based turbomachinery to become widely adopted and successful, a harmony between all elements of the machine must be achieved—bearingless technology enables rethinking the divide between motor and bearing for a more compact, simpler solution.

## Acknowledgements

This material is based upon work supported by the U.S. Department of Energy's Office of Energy Efficiency and Renewable Energy (EERE) under the Advanced Manufacturing Office, Emerging Research Exploration under award number DE-EE0009138.

## References

[1] M. T. White, G. Bianchi, L. Chai, S. A. Tassou, and A. I. Sayma, "Review of supercritical co2 technologies and systems for power generation," *Applied Thermal Engineering*, vol. 185, p. 116447, 2021.

[2] P. Rao, P. Sheaffer, Y. Chen, U. Karki, and P. Fitzgerald, "Us industrial and commercial motor system market assessment report volume 3: Energy saving opportunity," tech. rep., Lawrence Berkeley National Lab, 2022.

[3] J. Vaidya and E. Gregory, "High speed induction generator for applications in aircraft power systems," *SAE transactions*, pp. 1830–1836, 2004.

[4] S. Li, Y. Li, W. Choi, and B. Sarlioglu, "High-speed electric machines: Challenges and design considerations," *IEEE Transactions on Transportation Electrification*, vol. 2, no. 1, pp. 2–13, 2016.

[5] A. Morya, M. Moosavi, M. C. Gardner, and H. A. Toliyat, "Applications of wide bandgap (wbg) devices in ac electric drives: A technology status review," in *2017 IEEE International Electric Machines and Drives Conference (IEMDC)*, pp. 1–8, IEEE, 2017.

[6] S. A. Wright, R. F. Radel, M. E. Vernon, P. S. Pickard, and G. E. Rochau, "Operation and analysis of a supercritical co2 brayton cycle.," tech. rep., Sandia National Laboratories (SNL), Albuquerque, NM, and Livermore, CA , 2010.

[7] D. Kim, Y. Jeong, I. W. Son, and J. I. Lee, "A new windage loss model for s-co2 turbomachinery design," *Applied Sciences*, vol. 13, no. 13, p. 7463, 2023.

[8] V. Dostal, M. J. Driscoll, and P. Hejzlar, *A supercritical carbon dioxide cycle for next generation nuclear reactors*. PhD thesis, Massachusetts Institute of Technology, Department of Nuclear Engineering . . . , 2004.

[9] M. Branagan, D. Griffin, C. Goyne, and A. Untaroiu, "Compliant gas foil bearings and analysis tools," *Journal of Engineering for Gas Turbines and Power*, vol. 138, no. 5, p. 054001, 2016.

[10] M. Walker, D. D. Fleming, and J. J. Pasch, "Gas foil bearing coating behavior in environments relevant to s-co2 power system turbomachinery.," tech. rep., Sandia National Lab.(SNL-NM), Albuquerque, NM (United States), 2018.

[11] E. M. Clementoni, T. L. Cox, and M. A. King, "Off-nominal component performance in a supercritical carbon dioxide brayton cycle," *Journal of Engineering for Gas Turbines and Power*, vol. 138, no. 1, p. 011703, 2016.

[12] E. H. Maslen, G. Schweitzer, H. Bleuler, and M. Cole, *Magnetic bearings: theory, design, and application to rotating machinery*. Springer, 2009.

[13] K. Shalash and J. Schiffmann, "On the manufacturing of compliant foil bearings," *Journal of Manufacturing Processes*, vol. 25, pp. 357–368, 2017.

[14] Q. Gao, W. Chen, L. Lu, D. Huo, and K. Cheng, "Aerostatic bearings design and analysis with the application to precision engineering: State-of-the-art and future perspectives," *Tribology International*, vol. 135, pp. 1–17, 2019.

[15] L. San Andrés, T. A. Cable, Y. Zheng, O. De Santiago, and D. Devitt, "Assessment of porous type gas bearings: Measurements of bearing performance and rotor vibrations," in *Turbo Expo: Power for Land, Sea, and Air*, vol. 49842, p. V07BT31A031, American Society of Mechanical Engineers, 2016.

[16] D. Devitt, "Radial air bearings." `https://www.newwayairbearings.com/catalog/radial-air-bearings`. Online; accessed on: 2023-11-16.

[17] B. Ertas, J. Powers, K. Gary, D. Torrey, J. Zierer, P. Baehmann, V. Rallabandi, T. Adcock, N. Anandika, and R. A. Bidkar, "Test rig concept for evaluating the performance of a co2 immersed electro-mechanical rotor system utilizing gas bearings: Part-1 mechanical and electric machine design," in *Turbo Expo: Power for Land, Sea, and Air*, vol. 87073, p. V012T28A030, American Society of Mechanical Engineers, 2023.

[18] B. Ertas, "Additively manufactured compliant hybrid gas thrust bearing for sco2 turbomachinery: Design and proof of concept testing," in *Turbo Expo: Power for Land, Sea, and Air*, vol. 84218, p. V10AT25A017, American Society of Mechanical Engineers, 2020.

[19] B. Ertas, K. Gary, and A. Delgado, "Additively manufactured compliant hybrid gas thrust bearing for sco2 turbomachinery: Experimental evaluation and fluid-structure model predictions," in *Turbo Expo: Power for Land, Sea, and Air*, vol. 84218, p. V10AT25A018, American Society of Mechanical Engineers, 2020.

[20] G. Schweitzer, E. H. Maslen, *et al.*, *Magnetic bearings*. Springer, 2009.

[21] J. E. Cha, S. K. Cho, and J. I. Lee, "Operation test of the supercritical co2 compressor supported with active magnetic bearing," *Proceedings of the Korean Nuclear Society Autumn Meeting, Gyeongju, Korea*, 2016.

[22] L. Wolscht, K. Knobloch, E. Jacquemoud, and P. Jenny, "Dynamic simulation and experimental validation of a 35 mw heat pump based on a transcritical co2 cycle," in *The 5th European sCO2 Conference for Energy Systems*, pp. 93–105, EWL, University Duisburg-Essen, 2023.

[23] R. Shultz and A. Narayanaswamy, "Magnetic bearings for supercritical co2 turbomachinery," in *The 6th Internationl Supercritical CO2 Power Cycles Symposium*, 2018.

[24] D. Kim, S. Baik, and J. Lee, "Instability study of magnetic journal bearing under s-co2 condition," *Applied Sciences*, vol. 11, no. 8, p. 3491, 2021.

[25] M. T. White, G. Bianchi, L. Chai, S. A. Tassou, and A. I. Sayma, "Review of supercritical co2 technologies and systems for power generation," *Applied Thermal Engineering*, vol. 185, p. 116447, 2021.

[26] J. Moore, S. Cich, M. Day-Towler, and J. Mortzheim, "Development and testing of a 10 mwe supercritical co2 turbine in a 1 mwe flow loop," in *Turbo Expo: Power for Land, Sea, and Air*, vol. 84232, p. V011T31A018, American Society of Mechanical Engineers, 2020.

[27] S. A. Wright, T. M. Conboy, and G. E. Rochau, "Break-even power transients for two simple recuperated s-co2 brayton cycle test configurations.," tech. rep., Sandia National Lab.(SNL-NM), Albuquerque, NM (United States), 2011.

[28] L. M. Rapp, "Experimental testing of a 1mw sco2 turbocompressor.," tech. rep., Sandia National Lab.(SNL-NM), Albuquerque, NM (United States), 2019.

[29] J. Kang, A. Vorobiev, J. D. Cameron, S. C. Morris, R. Wackerly, K. Sedlacko, J. D. Miller, and T. J. Held, "10mw-class sco2 compressor test facility at university of notre dame," *The 4th European sCO2 Conference for Energy Systems*, 2021.

[30] D. Gerada, A. Mebarki, N. L. Brown, C. Gerada, A. Cavagnino, and A. Boglietti, "High-speed electrical machines: Technologies, trends, and developments," *IEEE transactions on industrial electronics*, vol. 61, no. 6, pp. 2946–2959, 2013.

[31] A. Tenconi, S. Vaschetto, and A. Vigliani, "Electrical machines for high-speed applications: Design considerations and tradeoffs," *IEEE Transactions on Industrial Electronics*, vol. 61, no. 6, pp. 3022–3029, 2013.

[32] J. Lähteenmäki *et al.*, *Design and voltage supply of high-speed induction machines*. Helsinki University of Technology, 2002.

[33] R. Van Millingen and J. Van Millingen, "Phase shift torquemeters for gas turbine development and monitoring," in *Turbo Expo: Power for Land, Sea, and Air*, vol. 79023, p. V005T15A003, American Society of Mechanical Engineers, 1991.

[34] D. Han, *Conducted common mode electromagnetic interference in wide bandgap semiconductor devices based DC-fed motor drives: Challenges and solutions*. The University of Wisconsin-Madison, 2017.

[35] A. Chiba, T. Fukao, O. Ichikawa, M. Oshima, M. Takemoto, and D. G. Dorrell, *Magnetic bearings and bearingless drives*. Elsevier, 2005.

[36] P. Hermann, "A radial active magnetic bearing having a rotating drive," *London Patent*, vol. 1, no. 500, p. 809, 1974.

[37] A. Chiba and T. Fukao, "Electric rotating machinery with radial position control windings and its rotor radial position controller," *Japan Patent*, vol. 2, no. 835, p. 522, 1989.

[38] A. Chiba, T. Deido, T. Fukao, and M. A. Rahman, "An analysis of bearingless ac motors," *IEEE Transactions on Energy Conversion*, vol. 9, no. 1, pp. 61–68, 1994.

[39] M. T. Bartholet, T. Nussbaumer, S. Silber, and J. W. Kolar, "Comparative evaluation of polyphase bearingless slice motors for fluid-handling applications," *IEEE Transactions on Industry Applications*, vol. 45, no. 5, pp. 1821–1830, 2009.

[40] Y. Okada, K. Dejima, and T. Ohishi, "Analysis and comparison of pm synchronous motor and induction motor type magnetic bearings," *IEEE Transactions on Industry Applications*, vol. 31, no. 5, pp. 1047–1053, 1995.

[41] C. Redemann, P. Meuter, A. Ramella, and T. Gempp, "30kw bearingless canned motor pump on the test bed," in *Seventh International Symp. on Magnetic Bearings, August 23-25, 2000, ETH Zurich*, 2000.

[42] T. Pei, D. Li, J. Liu, J. Li, and W. Kong, "Review of bearingless synchronous motors: Principle and topology," *IEEE Transactions on Transportation Electrification*, vol. 8, no. 3, pp. 3489–3502, 2022.

[43] M. Takemoto, H. Akagi, A. Chiba, and T. Fukao, "Torque and suspension force in a bearingless switched reluctance motor," *ieej transactions on industry applications*, vol. 124, no. 6, pp. 556–565, 2004.

[44] A. Chiba and T. Fukao, "Optimal design of rotor circuits in induction type bearingless motors," *IEEE Transactions on Magnetics*, vol. 34, no. 4, pp. 2108–2110, 1998.

[45] J. Chen, M. W. Johnson, A. Farhan, Z. Wang, Y. Fujii, and E. L. Severson, "Reduced axial length pole-specific rotor for bearingless induction machines," *IEEE Transactions on Energy Conversion*, vol. 37, no. 4, pp. 2285–2297, 2022.

[46] J. Chen, J. Zhu, and E. L. Severson, "Review of bearingless motor technology for significant power applications," *IEEE Transactions on Industry Applications*, vol. 56, no. 2, pp. 1377–1388, 2020.

[47] S. Silber, W. Amrhein, P. Bosch, R. Schob, and N. Barletta, "Design aspects of bearingless slice motors," *IEEE/ASME Transactions on Mechatronics*, vol. 10, no. 6, pp. 611–617, 2005.

[48] M. Neff, N. Barletta, and R. Schob, "Bearingless centrifugal pump for highly pure chemicals," in *Proc. 8th Int. Symp. Magnetic Bearings*, pp. 283–287, 2002.

[49] G. Munteanu, A. Binder, and T. Schneider, "Loss measurement of a 40 kw high-speed bearingless pm synchronous motor," in *2011 IEEE Energy Conversion Congress and Exposition*, pp. 722–729, Sept 2011.

[50] Z. Liu, A. Chiba, Y. Irino, and Y. Nakazawa, "Optimum pole number combination of a buried permanent magnet bearingless motor and test results at an output of 60 kw with a speed of 37000 r/min," *IEEE Open Journal of Industry Applications*, vol. 1, pp. 33–41, 2020.

[51] D. Dietz and A. Binder, "Comparison between a bearingless pm motor with separated and combined winding for torque and lateral force generation," in *2019 21st European Conference on Power Electronics and Applications (EPE'19 ECCE Europe)*, pp. P–1, IEEE, 2019.

[52] A. Khamitov, W. Gruber, G. Bramerdorfer, and E. L. Severson, "Comparison of combined winding strategies for radial nonsalient bearingless machines," *IEEE Transactions on Industry Applications*, vol. 57, no. 6, pp. 6856–6869, 2021.

[53] A. Khamitov and E. L. Severson, "Design of multi-phase combined windings for bearingless machines," *IEEE Transactions on Industry Applications*, vol. 59, no. 3, pp. 3243–3255, 2023.

[54] I. Ahmed and E. L. Severson, “Bearingless generator design and optimization for high-speed applications,” in *2021 IEEE Energy Conversion Congress and Exposition (ECCE)*, pp. 4562–4569, IEEE, 2021.

[55] D. Kepsu, R. P. Jastrzebski, and O. Pyrhönen, “Modeling of a 30 000 rpm bearingless spm drive with loss and thermal analyses for a 0.5 mw high-temperature heat pump,” *IEEE Transactions on Industry Applications*, vol. 57, no. 6, pp. 6965–6976, 2021.

[56] D. Kepsu, R. P. Jastrzebski, O. Pvrhönen, and E. Kurvinen, “Scalability of spm bearingless high - speed motor for 180 – 280 kw applications,” in *2019 IEEE International Electric Machines and Drives Conference (IEMDC)*, pp. 329–335, 2019.

[57] H. Sugimoto, M. Miyoshi, and A. Chiba, “Axial vibration suppression by field flux regulation in two-axis actively positioned permanent magnet bearingless motors with axial position estimation,” *IEEE Transactions on Industry Applications*, vol. 54, no. 2, pp. 1264–1272, 2018.

[58] Z. Wang, X. Cao, Z. Deng, and K. Li, “Modeling and characteristic investigation of axial reluctance force for bearingless switched reluctance motor,” *IEEE Transactions on Industry Applications*, vol. 57, no. 5, pp. 5215–5226, 2021.

[59] H. Mitterhofer, G. Jungmayr, W. Amrhein, and K. Davey, “Coaxial tilt damping coil with additional active actuation capabilities,” *IEEE Transactions on Industry Applications*, vol. 54, no. 6, pp. 5879–5887, 2018.

[60] J. Chen, Y. Fujii, M. W. Johnson, A. Farhan, and E. L. Severson, “Optimal design of the bearingless induction motor,” *IEEE Transactions on Industry Applications*, vol. 57, no. 2, pp. 1375–1388, 2021.